

Bayesian optimal design using stochastic gradient optimisation and Fisher information gain

Sophie Harbisher, Colin S Gillespie and Dennis Prangle
School of Mathematics Statistics and Physics, Newcastle University, UK

Abstract

Finding high dimensional designs is increasingly important in applications of experimental design, but is computationally demanding under existing methods. We introduce an efficient approach applying recent advances in stochastic gradient optimisation. To allow rapid gradient calculations we work with a computationally convenient utility function, the trace of the Fisher information. We provide a decision theoretic justification for this utility, analogous to work by Bernardo (1979) on the Shannon information gain. Due to this similarity we refer to our utility as the Fisher information gain. We compare our optimisation scheme, SGO-FIG, to existing state-of-the-art methods and show our approach is quicker at finding designs which maximise expected utility, allowing designs with hundreds of choices to be produced in under a minute in one example.

1 Introduction

Selecting a good design for an experiment can be crucial to extracting useful information and controlling costs. Applications include medical studies (Amzal et al., 2006), epidemic modelling (Cook et al., 2008), pharmacokinetics (Ryan et al., 2014; Overstall and Woods, 2017) and ecology (Gillespie and Boys, 2019). In modern applications it is increasingly feasible to take a large

number of measurements, for example placing sensors (Krause et al., 2009) or making observations in a numerical integration problem (Oates et al., 2019). Therefore high dimensional designs are increasingly relevant. However most methods for optimal design are expensive in the high dimensional setting, so there is a need for more efficient and scalable methods.

We focus on the Bayesian approach to optimal experimental design, which takes into account existing knowledge and uncertainty about the process being studied before the experiment is undertaken. In this framework an experimenter must select a design. They then receive some utility based on the outcome of the experiment. The aim is to select the design which maximises expected utility given the experimenter’s beliefs before the experiment takes place. Mathematically this is an optimisation problem. A practical challenge is that the expected utility to be optimised usually cannot be calculated exactly. Instead only random estimates can be produced through simulation. We approach the problem by applying methods from the machine learning literature for high dimensional optimisation in similar settings: automatic differentiation and adaptive variants of stochastic gradient descent. These rely on being able to estimate the gradient of the expected utility with respect to the design. Therefore our methods are relevant to problems where there is a continuous space of possible designs.

For many utility functions it is expensive to estimate utilities or their gradients. For instance, a single utility evaluation often requires performing some aspect of Bayesian inference for simulated data using a Monte Carlo calculation. Therefore we focus on a utility function which is particularly computationally convenient as it is often available in closed form: the trace of the Fisher information. This is commonly used in classical optimal design, but is often criticised in the Bayesian experimental design literature as effectively only relying on an approximation to the posterior (see Section 2 for more discussion). However Walker (2016) shows that it has an information theoretic justification. We provide a further justification of this utility as a Bayesian approach, by noting that there is a derivation directly from the first principles of decision theory. The argument is analogous to that of Bernardo (1979) supporting the use of the Shannon information gain utility. Due to this similarity, we refer to our utility as the *Fisher information gain* (FIG). Our derivation is based on judging the quality of a parameter estimate through the Hyvärinen score (Hyvärinen, 2005), rather than through the logarithmic score as in Bernardo (1979).

We compare our optimisation scheme, SGO-FIG, to existing state-of-the-

art methods such as the algorithm of Müller (1999) and ACE (Overstall and Woods, 2017), also using the FIG utility. Our approach is quicker at finding designs which are local maxima of expected utility, and allows designs with hundreds of choices to be produced in under a minute. A potential drawback of our method is that in one example it often converges to poor local maxima. We show how post-processing methods from Overstall and Woods (2017) can be used to find the overall optimal design. In our conclusion, Section 8 we present general recommendations of how to combine SGO-FIG with post-processing.

Similar gradient-based optimisation approaches to ours have been explored previously. Pronzato and Walter (1985) optimise the expected determinant of the Fisher information using analytically derived gradients. Huan and Marzouk (2013, 2014) optimise expected Shannon information using gradients (either derived analytically or based on finite differences) for a biased numerical approximation to the utility. The novelty of our approach is to use recently developed adaptive stochastic gradient algorithms and automatic differentiation frameworks, as well as a utility function chosen to allow cheap calculation of unbiased gradient estimates.

To summarise, the main contribution of our paper is an efficient algorithm for high dimensional Bayesian optimal design using stochastic gradient optimisation. The algorithm relies on a particular utility function: Fisher information gain. A secondary contribution of our work is a decision theoretic justification for its use. To save space, the latter contribution is mainly discussed in the appendix.

The remainder of the paper is structured as follows. Section 2 presents background on Bayesian experimental design, including common utility functions, the role of decision theory and existing computational methods. Section 3 describes the utility function we use, Fisher information gain. Section 4 presents our algorithm for optimal design. Sections 5 – 7 present three example applications, including a comparison of our algorithm to existing methods. Code to illustrate all of these applications is available at github.com/SophieHarbisher/SGO-FIG. Finally, Section 8 concludes with a discussion.

2 Bayesian experimental design

Optimal experimental design concerns the following problem. An experimenter must select a design τ . The experiment produces data y with likelihood $f(y|\theta; \tau)$, where θ is a vector of unknown parameters. The goal is to select the design which optimises some notion of the quality of the experiment, typically based on its informativeness and its cost.

The Bayesian approach to experimental design involves selecting a function $\mathcal{U} = \mathcal{U}(\tau, \theta, y)$, giving the utility of selecting design τ given observations y and true parameters θ . (As we shall see, some choices of \mathcal{U} do not depend on all these possible inputs.) We try to maximise the *expected utility* of τ i.e. the prior predictive utility

$$\mathcal{J}(\tau) = \mathbb{E}_{\theta \sim \pi(\theta), y \sim f(y|\theta; \tau)}[\mathcal{U}(\tau, \theta, y)], \quad (1)$$

where $\pi(\theta)$ is the prior density for θ . The optimal design τ^* is that maximising $\mathcal{J}(\tau)$. Throughout we consider the case where a unique maximum exists, although much of the methodology will remain useful when this is not the case.

This section reviews relevant details of Bayesian experimental design. See Chaloner and Verdinelli (1995) and Ryan et al. (2016) for more comprehensive surveys. First, Section 2.1 introduces some useful notation. Section 2.2 summarises some common choices of utility function, and Section 2.3 describes a particularly principled approach: deriving it with decision theory. Section 2.4 reviews existing computational methods for estimating the optimal design.

2.1 Notation

As usual in Bayesian statistics, we will make use of the posterior density and the prior predictive density for y . In our setting both depend on the experimental design τ ,

$$\pi(\theta|y; \tau) = \pi(\theta)f(y|\theta; \tau)/\pi(y; \tau), \quad (2)$$

$$\pi(y; \tau) = \mathbb{E}_{\theta \sim \pi(\theta)}[f(y|\theta; \tau)]. \quad (3)$$

We will also make use of the Fisher information matrix,

$$\mathcal{I}(\theta; \tau) = \mathbb{E}_{y \sim f(y|\theta; \tau)}[u(y, \theta; \tau)u(y, \theta; \tau)^T], \quad (4)$$

which is based on the score function,

$$u(y, \theta; \tau) = \nabla_{\theta} \log f(y|\theta; \tau). \quad (5)$$

We will focus on models where both of these are well defined.

We concentrate on the case where $\tau = (\tau_1, \dots, \tau_d) \in \mathcal{T} \subseteq \mathbb{R}^d$ i.e. a design is a fixed number, d , of real-valued quantities. Such a design typically represents times or locations of measurements. We will typically assume there are p parameters $\theta_1, \theta_2, \dots, \theta_p$ and that y is a vector of n observations y_1, y_2, \dots, y_n .

2.2 Common utility functions

Ideally a specific utility function for the situation at hand could be chosen, perhaps by eliciting preferences over different (τ, θ, y) combinations from the experimenter (e.g. Wolfson et al., 1996). However this is often infeasible in practice. Instead several generic choices of utility have been proposed, including: scalar summaries of posterior precision or the difference between θ and $\mathbb{E}[\theta|y]$ (the posterior mean); information theoretic choices; utilities based on predicting future observations. Ryan et al. (2016) describe these utilities in more detail, and refer to them as *fully Bayesian* as they are functionals of the posterior distribution $\pi(\theta|y; \tau)$.

Producing good estimates of posterior quantities can be computationally expensive. Hence another set of generic utility choices are based on cruder posterior approximations, in particular Gaussian approximations using $\mathcal{I}(\theta; \tau)^{-1}$, the inverse of the Fisher information matrix (4), as the variance matrix (Chaloner and Verdinelli, 1995). The utility can then be taken to be a scalar summary of $\mathcal{I}(\theta; \tau)$. This corresponds to using alphabet optimality criteria from classical experimental design (Box, 1982). Such utilities include $\text{tr} \mathcal{I}(\theta; \tau)$ (T-optimality), $\det \mathcal{I}(\theta; \tau)$ (D-optimality) and $-\text{tr} \mathcal{I}(\theta; \tau)^{-1}$ (A-optimality). Ryan et al. (2016) refer to these as *pseudo-Bayesian* as they are not functionals of the posterior.

Remark 1. *The distinction between pseudo and fully Bayesian utility functions is not as clear cut as it appears. In particular, Section 3 will present an example where a fully Bayesian and a pseudo-Bayesian utility (under the preceding definitions) are equivalent, in the sense of always producing the same expected utility function up to an additive constant, and hence the same optimal design. We explore this issue further in Appendix A.*

A utility of particular interest later is *Shannon information gain* (SIG),

$$\mathcal{U}_{SIG}(\tau, \theta, y) = \log \pi(\theta|y; \tau) - \log \pi(\theta) \quad (6)$$

$$= \log f(y|\theta; \tau) - \log \pi(y; \tau) \quad (7)$$

A common SIG estimate replaces $\pi(y; \tau)$ in (7) with a Monte Carlo estimate

$$\hat{\pi}(y; \tau) = \frac{1}{L} \sum_{\ell=1}^L f(y|\theta^{(\ell)}; \tau), \quad (8)$$

where $\theta^{(\ell)}$ are independent draws from the prior. A typical choice of L is 1000 (Overstall and Woods, 2017), which makes each utility evaluation somewhat computationally expensive. Furthermore, some approximation error is introduced. In general, numerical estimation of most fully Bayesian utility functions involves a similar mixture of computational cost and approximation error (see e.g. Ryan et al., 2016 and Overstall and Woods, 2017 for details).

2.3 Bayesian decision theory

Lindley (1972), following Raiffa and Schlaifer (1961), proposed viewing experimental design as a decision problem. As in the general framework at the start of Section 2, the experimenter selects a design τ and the experiment produces data y given parameters θ with an assumed prior distribution. Following this, the experimenter selects an action a based on observing y (but not θ). Their preferences are represented by a function $\mathcal{V}(a, \theta, y, \tau)$, which we will refer to as the *base utility*.

The utility \mathcal{U} required for Bayesian experimental design can be derived by assuming that the optimal action a (which we assume exists) is always taken, giving

$$\mathcal{U} = \max_a \mathbb{E}_{\theta \sim \pi(\theta|y; \tau)} [\mathcal{V}(a, \theta, y, \tau)].$$

(Note this is a case where the utility \mathcal{U} depends on τ and y only.) In principle the base utility could be elicited from the experimenter’s preferences. However this is often not possible and instead a generic function can be used. For instance a simple possibility is to let a be a point estimate of θ and use $\mathcal{V} = (a - \theta)^T(a - \theta)$ i.e. mean squared error. See Chaloner and Verdinelli (1995) for further discussion.

Bernardo (1979) proposed that a instead be an estimated density for θ . The utility can then be based on a *strictly proper scoring rule*, a functional

for evaluating the quality of density estimates. Bernardo showed that this framework allows a decision theoretic derivation of Shannon information gain. We summarise the argument in Appendix A.

2.4 Existing computational methods

Below we discuss two popular algorithms for Bayesian experimental design, which we use in our comparisons: the Müller and ACE algorithms. Many other algorithms have been proposed. For example, Ryan et al. (2014) look at high dimensional designs with a low dimensional parametric form, Price et al. (2018) use evolutionary algorithms, and Gillespie and Boys (2019) perform a sophisticated search on a discrete grid of designs.

Müller algorithm Müller (1999) performs optimal design using Markov Chain Monte Carlo (see Amzal et al., 2006 and Kück et al., 2006 for similar approaches using sequential Monte Carlo.) The target density is

$$h(\tau, \theta_1, \dots, \theta_J, y_1, \dots, y_J) \propto \prod_{j=1}^J \mathcal{U}(\tau, \theta_j, y_j) \pi(\theta_j) f(y_j | \theta_j; \tau).$$

The marginal density for τ is proportional to a power of the expected utility, $\mathcal{J}(\tau)^J$. Hence the mode of τ under this marginal is the optimal design. Estimating the mode from MCMC samples can be non-trivial, especially for high dimensional designs. Taking larger values of J makes the mode easier to identify, but increases the computational cost of each iteration.

The Müller algorithm uses Metropolis-Hastings to sample from the target distribution. To draw a proposal, first τ^* is sampled from a proposal kernel. Then (θ_j^*, y_j^*) pairs are sampled independently from $\pi(\theta) f(y | \theta; \tau^*)$. In our implementation we sample $\tau^* \sim N(\tau, \sigma_{RW}^2 I)$. Therefore the tuning choices we require are J and σ_{RW} .

Approximate co-ordinate exchange (ACE) The ACE algorithm (Overstall and Woods, 2017) consists of two phases. Phase I is referred to as coordinate exchange. It loops over the components of the design, updating each in turn. To perform an update, designs are selected from the one dimensional search space (in which the current component only is updated) and Monte Carlo estimates of expected utility calculated. A Gaussian process is fitted to

the expected utility estimates and used to propose an improved value for the design component under consideration. This is accepted or rejected based on a Bayesian test of whether it improves expected utility, using a large number of simulations under the current and proposed designs.

Phase II is referred to point exchange. It considers whether the design output by phase I can be improved by replacing some components of the design with replicates of other components. New designs are proposed in a greedy fashion, replicating the design point which would yield the largest improvement in estimated expected utility, then removing the point which would result in the least reduction of the estimated expected utility. Similarly to phase I, the proposed design is then accepted based on a Bayesian test of whether expected utility is improved, after sampling utilities under the existing and candidate designs.

ACE can converge to local optima so the authors suggest running the algorithm multiple times and selecting the design which returns the highest expected utility. These runs can be performed in parallel to reduce computation time. The algorithm is implemented in the `acebayes` R package (Overstall et al., 2017). The package allows ACE phase II to be run separately, so it can be used to post-process designs from any algorithm.

3 Fisher information gain

Section 3.1 introduces the Fisher information gain utility, and discusses its properties, with further details given in Appendix A. Section 3.2 discusses evaluating it computationally.

3.1 Definition and properties

Walker (2016) proposes maximising the following objective function for optimal design:

$$\mathcal{J}_{FIG}(\tau) = \mathbb{E}_{\theta \sim \pi(\theta)}[\text{tr } \mathcal{I}(\theta; \tau)]. \quad (9)$$

Under the framework of Section 2.2, the utility function used is

$$\mathcal{U}_{FIG} = \text{tr } \mathcal{I}(\theta; \tau), \quad (10)$$

corresponding to classical T-optimality. We'll refer to this as the *Fisher information gain* (FIG) due to an analogy with SIG discussed in Appendix A.

Remark 2. *One potential drawback of the FIG utility is that it is not invariant to reparameterisation. We discuss this further in Section 4.4.*

Since the right hand side of (10) does not involve y , the FIG utility is not a functional of the posterior, and therefore is pseudo-Bayesian under the terminology of Ryan et al. (2016). However Walker (2016) shows that \mathcal{J}_{FIG} also results (up to an additive constant) from using utilities which are functionals of the posterior (detailed in Section A.4 of the appendix). As noted in Remark 1, hence an expected utility equivalent to \mathcal{J}_{FIG} can be derived from both pseudo-Bayesian and fully-Bayesian utility functions.

A contribution of our paper is to provide stronger theoretical support for \mathcal{J}_{FIG} , by extending the theoretical argument of Bernardo (1979) supporting SIG to produce the following results.

Result 1. *The expected utility \mathcal{J}_{FIG} can be derived from Bayesian decision theory using the negative Hyvärinen score (Hyvärinen, 2005) as the base utility.*

The background and proof of this result are presented in Appendix A. This also discusses how the various utilities discussed by Walker (2016) correspond to information theoretic quantities derived from the Hyvärinen score. The most computationally convenient to use in practice is \mathcal{U}_{FIG} , as discussed in the next section.

3.2 Evaluation of the Fisher information gain

An advantage of the FIG utility is that for many models the Fisher information is available in closed form. This avoids the computational cost and approximation error associated with many alternative utilities, discussed in Section 2.2. (When a closed form is not available unbiased Monte Carlo estimation is possible. See Appendix E for details of this case.)

We give details here of one general case which we will use in some later examples. Consider a model with observation vector $y \sim N(x(\theta, \tau), \Sigma(\tau))$. That is, the observations are true values $x(\theta, \tau)$ plus normal noise, which may be correlated. The entry in row i column j of the associated Fisher information matrix is (see e.g. Miller, 1974, section V, equation (4.4))

$$\mathcal{I}_{i,j}(\theta; \tau) = v_i(\theta, \tau)^T \Sigma(\tau)^{-1} v_j(\theta, \tau),$$

where v_i is the vector $\frac{\partial}{\partial \theta_i} x(\theta, \tau)$ of elementwise derivatives of x . Thus

$$\text{tr } \mathcal{I}(\theta; \tau) = \sum_{i=1}^p v_i(\theta, \tau)^T \Sigma(\tau)^{-1} v_i(\theta, \tau). \quad (11)$$

Remark 3. *Under the normal observation model, replacing $\Sigma(\tau)$ with $\kappa \Sigma(\tau)$ for a scalar $\kappa > 0$ only affects the FIG utility by a constant of proportionality, and so does not change the optimal design.*

4 Maximising expected Fisher information gain

We have described how the FIG utility can easily be numerically evaluated. As we shall see, gradient calculations are also straightforward. This is in contrast to many other utility functions for Bayesian experimental design, where every utility evaluation involves high computational cost or approximation error (see Section 2.2), and gradient information is not easily available. These helpful properties of the FIG utility means it can be used with powerful *stochastic gradient optimisation* methods to maximise the expected utility $\mathcal{J}_{FIG}(\tau)$, as we outline in this section.

Section 4.1 presents our algorithm for Bayesian optimal design and background on the methods it uses. The algorithm requires unbiased estimates of the gradient of $\mathcal{J}_{FIG}(\tau)$, and Section 4.2 discusses calculating these. Section 4.3 is on optimisation under constraints to the space of designs, and Section 4.4 is about optimising a weighted version of the FIG, and how this is helpful to learn information about all the parameters rather than a subset of them.

Note that throughout the paper we use ∇ to represent gradient with respect to τ . When differentiation with respect to another vector is required we add a subscript e.g. ∇_θ .

4.1 Optimisation algorithm

Algorithm 1 summarises our SGO-FIG algorithm to maximise $\mathcal{J}_{FIG}(\tau)$. We typically run this for a fixed number of iterations. Alternatively it could be run until a convergence condition is reached. For example $\mathcal{J}_{FIG}(\tau)$ could be estimated at each iteration and a moving average recorded, with the algorithm terminating if the minimum moving average value is not beaten for a prespecified number of iterations.

Algorithm 1 SGO-FIG: Stochastic gradient optimisation of expected Fisher information gain

Input: Initial design τ_0 , number of iterations n , batch size K (used in gradient estimation).

Loop over $t = 0, 1, 2, \dots, n - 1$ or until a convergence condition is reached:

1. Calculate g_t , an estimate of $\nabla \mathcal{J}_{FIG}(\tau)$ at $\tau = \tau_t$, using (12) from Section 4.2.
(This requires a closed form expression for $\mathcal{I}(\theta; \tau)$. See Appendix E for alternatives when this is not available.)
2. Get τ_{t+1} by calling the update rule of a stochastic gradient optimisation algorithm with current state τ_t and gradient estimate g_t . We use the update rule of the Adam algorithm (Kingma and Ba, 2015).

The remainder of this section briefly discusses the background to the optimisation methods used in step 2 of SGO-FIG. Our aim is to maximise $\mathcal{J}_{FIG}(\tau)$ although we cannot compute this function exactly. This is possible using iterative steps of stochastic gradient optimisation methods. A straightforward iterative update is

$$\tau_{t+1} = \tau_t + a_t g_t,$$

where g_t is an unbiased estimate of $\nabla \mathcal{J}_{FIG}(\tau)$ at $\tau = \tau_t$ and a_t is a decreasing *learning rate* sequence. For unbiased gradient estimates and an appropriate a_t sequence, convergence to a local optimum is guaranteed. See Kushner and Yin (2003) and Bottou et al. (2018) for an overview of the theory. However, selecting the learning rate sequence in advance is a considerable tuning challenge which has a large effect on the speed of convergence.

In the last decade many adaptive stochastic gradient optimisation algorithms have been proposed (Ruder, 2016). These select the learning rate adaptively based on the observed g_t s to speed convergence. Furthermore, a separate learning rate is used for each entry of the τ vector. Various algorithms of this form are in common use and we use the popular Adam (“adaptive moments”) algorithm, which produces state-of-the-art empirical performance on optimisation problems in deep learning with millions of unknowns or more

(Kingma and Ba, 2015). (Adam is technically a minimisation method, so we use it to minimise $-\mathcal{J}_{FIG}(\tau)$.) An appealing feature of Adam is that it often does not require tuning, with the default choices performing well in many situations. We experimented with varying the default tuning choices for the examples in this paper and found no improvement.

4.2 Gradient estimation

SGO-FIG requires unbiased estimates of $\nabla \mathcal{J}_{FIG}(\tau)$. From the definition of $\mathcal{J}_{FIG}(\tau)$, (9), and assuming weak regularity conditions (see Appendix D) to allow interchange of differentiation and expectation,

$$\nabla \mathcal{J}_{FIG}(\tau) = \mathbb{E}_{\theta \sim \pi(\theta)}[\nabla \text{tr} \mathcal{I}(\theta; \tau)].$$

A closed form of the Fisher information is often available (see Appendix E for when this is not the case). In this case an unbiased Monte Carlo gradient estimate is

$$\widehat{\nabla \mathcal{J}_{FIG}(\tau)} = \frac{1}{K} \sum_{k=1}^K \nabla \text{tr} \mathcal{I}(\theta^{(k)}; \tau), \quad (12)$$

where $\theta^{(k)}$ are independent draws from the prior. Using a larger Monte Carlo batch size K reduces the variance of the estimates but increases computational cost.

Typically we can calculate this gradient estimate using automatic differentiation (Baydin et al., 2017). Our code does this using the Tensorflow framework (Abadi et al., 2016). We manually compute the function to be differentiated, $\text{tr} \mathcal{I}(\theta; \tau)$. See Sections 5–7 for some examples. Deriving $\text{tr} \mathcal{I}(\theta; \tau)$ can itself involve lengthy differentiation, and there may be scope for future work to avoid this using advanced automatic differentiation methods.

4.3 Optimisation under constraints

We often wish to optimise the expected utility under a constraint: $\tau \in \mathcal{T} \subset \mathbb{R}^p$. For the application in this paper, constrained optimisation was possible by the simple pragmatic approach of adding a large penalty to expected utilities for $\tau \notin \mathcal{T}$, whose gradient moves designs back towards the feasible space \mathcal{T} .

In more complex settings this penalisation method may not suffice. A more sophisticated alternative is to compose each stochastic gradient optimisation update with a projection operation into \mathcal{T} (Kushner and Yin, 2003).

4.4 Optimisation using weights

The FIG utility can be written as

$$\text{tr } \mathcal{I}(\theta; \tau) = \sum_{i=1}^p \mathbb{E}_{y \sim f(y|\theta; \tau)} \left[u_i(y, \theta; \tau)^2 \right], \quad (13)$$

where $u_i = \frac{\partial}{\partial \theta_i} \log f(y|\theta; \tau)$ is the i th element of the score function u . An alternative utility is to use a weighted version of the sum in (13). We now show that this is equivalent to rescaling the parameters. (This shows that the FIG is not invariant under reparameterisation, as mentioned in Remark 2.)

Consider $\vartheta = W\theta$ where W is a diagonal weight matrix with diagonal entries w_1, w_2, \dots, w_p , all positive. Let w represent the vector of these weights. Then it is easy to show that

$$\text{tr } \mathcal{I}(\vartheta; \tau) = \text{tr}[\mathcal{I}(\theta; \tau)W^{-2}] = \sum_{i=1}^p \mathbb{E}_{y \sim f(y|\theta; \tau)} \left[u_i(y, \theta; \tau)^2 / w_i^2 \right]. \quad (14)$$

The corresponding expected utility is

$$\mathcal{J}_{FIG}(\tau; w) = \mathbb{E}_{\theta \sim \pi(\theta)} \text{tr} [\mathcal{I}(\theta; \tau)W^{-2}].$$

When there is no natural parameter scale to use, we argue it is reasonable to weight the parameters so that each contributes a comparable amount to the sum in (14). Otherwise optimal design may concentrate on maximising informativeness for a subset of parameters: those with the largest contributions (see Table 1 later for an example).

In Appendix B we present Algorithm 2, which adaptively learns weights with the property just described, and optimises (14). We found this algorithm has good empirical performance. However, its convergence is not guaranteed. To ensure convergence, one can use Algorithm 2 to pick reasonable weights, and then run Algorithm 1 using rescaled parameters ϑ . See Appendix B for further details.

5 Death model example

Several authors have investigated experimental design for the simple death process (Renshaw, 1993; Cook et al., 2008; Gillespie and Boys, 2019). To

illustrate our method, we consider this setting with a single observation time, τ . In this scenario the observation model is $Y \sim \text{Bin}(N, \lambda)$ where $\lambda = \exp(-\theta\tau)$. Here N is a known constant and θ is the parameter of interest.

The Fisher information for this model can be derived from two standard results. First, the Fisher information for $Y \sim \text{Bin}(N, \phi)$ is $\mathcal{I}_\phi(\phi) = \frac{N}{\phi(1-\phi)}$. Secondly, a reparameterisation $\varphi = \varphi(\phi)$ produces $\mathcal{I}_\varphi(\varphi) = \mathcal{I}_\phi(\phi) \left(\frac{d\phi}{d\varphi}\right)^2$. Hence for the death model we have

$$\mathcal{I}_\theta(\theta) = \frac{N\tau^2\lambda}{1-\lambda} = \frac{N\tau^2\exp(-\theta\tau)}{1-\exp(-\theta\tau)}.$$

Since this is scalar, the expected FIG utility is $\mathcal{J}_{FIG}(\tau) = \mathbb{E}_\theta[\mathcal{I}_\theta(\theta)]$. Following Cook et al. (2008), we take $N = 50$ and a log normal $LN(0.005, 0.01)$ prior distribution for θ . In this example the expected utility is a univariate integral, so near-exact calculation by numerical integration is possible. Figure 1a shows the resulting utility surface, and the optimal observation time $\tau^* \approx 1.61$. (Gillespie and Boys (2019) report the same optimal design to 2 decimal places, despite using a different utility: posterior precision. An explanation is that Fisher information is an approximation to posterior precision.)

Figure 1b shows 11 independent runs of SGO-FIG with initial τ values of $0, 1, 2, \dots, 10$, and a batch size of $K = 1$. (In practice rather than $\tau = 0$ we used a small positive value to avoid numerical issues.) Regardless of the initial τ value, SGO-FIG quickly locates the optimal design. As would be expected, the closer the initial value is to τ^* , the quicker the algorithm converges. Each analysis uses 10,000 iterations, which runs in only a few seconds for this simple example.

6 Pharmacokinetic example

This section contains simulation studies using a pharmacokinetic model. The goal is to investigate the performance of our optimisation method and compare it with existing methods. We focus on also using the FIG utility in the other methods to give a fair comparison.

Throughout we compare the methods based on how many utility evaluations they perform. For SGO-FIG each utility evaluation also has an associated gradient evaluation calculation, performed using automatic differentiation. Due to this extra cost we also comment on the time taken for

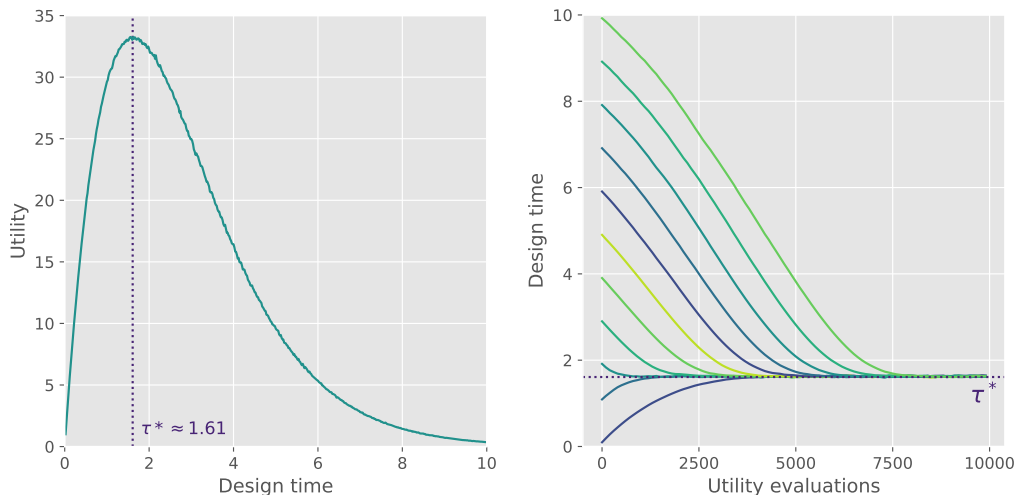


Figure 1: Death model plots (a) The utility surface. (b) Trace plots of observation time τ against computational cost (measured in utility gradient evaluations) for 11 independent runs of SGO-FIG. The optimal design τ^* is shown by the dotted line.

the different methods, although this is an imperfect comparison as it is influenced by implementation details of the methods, such as what programming language was used.

Model We assume that drug concentration, y_j , at time τ_j (in hours) is distributed as

$$y_j \sim N(x(\theta, \tau_j), \sigma^2),$$

$$\text{where } x(\theta, \tau_j) = \frac{D\theta_2(\exp[-\theta_1\tau_j] - \exp[-\theta_2\tau_j])}{\theta_3(\theta_2 - \theta_1)},$$

and $D = 400$. Concentrations at different times are assumed to be independent. This is a modification of a model from Ryan et al. (2014) and Overstall and Woods (2017), removing a multiplicative noise term for simplicity.

Following this earlier work we assume independent log normal prior distributions

$$\theta_1 \sim LN(\log 0.1, 0.05), \theta_2 \sim LN(\log 1, 0.05), \theta_3 \sim LN(\log 20, 0.05),$$

Method	Relative change		
	θ_1	θ_2	θ_3
Unweighted	+218%	-93%	-13%
Weighted	+56%	+125%	+109%

Table 1: Relative change in the individual components of the sum (13) for each parameter after SGO-FIG optimisation of weighted and unweighted objectives for the pharmacokinetic example. Tuning choices are described in Table 2.

and aim to find 15 observation times in $[0, 24]$. Also we treat $\sigma = 0.1$ as known. Previous work required consecutive observations to be at least 15 minutes apart. We do not enforce this condition as its implementation would vary between methods making it difficult to draw fair conclusions.

Methods The FIG utility for this model can be calculated using (11). See Appendix C for details. When implementing the algorithms, we found no need to use constrained optimisation as the designs remained in the interval $[0, 24]$ in any case.

The three terms in the sum representation of the FIG (13) are on widely different scales for this example. Table 1 shows that using SGO-FIG directly on this utility only increases the utility contribution for one parameter. Hence we use a weighted FIG (14) instead. After a short pilot run using adaptive weights (i.e. Algorithm 2), weights of $w = (5 \times 10^5, 3 \times 10^3, 70)$ were selected. In the remainder of this section all methods use parameters scaled by these weights. Table 1 shows that SGO-FIG on the weighted FIG objective increases the utility contribution for all parameters.

Table 2 contains details of the algorithms we compare and their tuning choices. We sampled 100 initial designs from a uniform distribution over the search space. Each algorithm is run from each of these initial designs. We also investigate post-processing the results from each method using the ACE phase II algorithm (under its default tuning choices from Overstall and Woods, 2017).

Results First we investigated the cost of evaluating the FIG and SIG utilities. As discussed earlier, we expect SIG evaluation to be slower as it

Method	Tuning choices
ACE (phase I)	Defaults, as given by Overstall and Woods (2017)
SGO-FIG	1.87×10^7 iterations, $K = 1$ (other K values discussed below)
Müller 1	$J = 1$, 1.87×10^7 iterations, $\sigma_{RW}^2 = 1 \times 10^{-2}$
Müller 2	$J = 2$, 9.35×10^6 iterations, $\sigma_{RW}^2 = 2 \times 10^{-4}$

Table 2: Settings for the algorithms used in the pharmacokinetic model simulation studies. The number of utility evaluations used in each aims to equal the default computational cost of the ACE algorithm (1.87×10^7 iterations). See Section 2.4 for the interpretation of the Müller tuning parameters.

requires computing a Monte Carlo estimate (8). In ACE, the mean time to produce 1000 utility evaluations was 0.008 seconds for FIG compared to 0.082 seconds for SIG. Hence FIG produces roughly a 10 times speed-up in utility evaluation compared to SIG. (This is despite our FIG calculations within ACE being performed in user-supplied R code, while more efficient built-in C code is used for SIG.)

Figure 2 shows expected utilities returned by each optimal design method. Müller makes only a small improvement on the initial designs. SGO-FIG makes a larger improvement but does worse than ACE. Post-processing helps all the methods, with SGO-FIG results now generally the best, but occasionally extremely poor (about 10% of results have expected utility close to 2.5).

Speed of convergence is also of interest. Figure 3 is a trace plot of utilities during the execution of the ACE and SGO-FIG algorithms. SGO-FIG converges much quicker than ACE (taking only around 10^4 iterations), while ACE does not appear to have converged after the full computational budget. However SGO-FIG can converge to several different expected utilities, typically achieving a worse value than ACE.

For a fixed number of utility evaluations ACE was much quicker to execute than the other methods. For one particular initial design, approximate times were (in seconds) ACE 130, SGO-FIG 7,800, Müller 1 9,000, Müller 2 4,500. (The cost of our implementation of the Müller algorithm is dominated by non-utility calculations for each iteration, which is why computation time is halved when using half as many iterations.) However SGO-FIG takes only 40s to reach 10^4 utility evaluations, at which point it has effectively converged.

Figure 4 summarises the designs returned by the algorithms. The Müller algorithm produces designs approximately uniformly spaced across the design

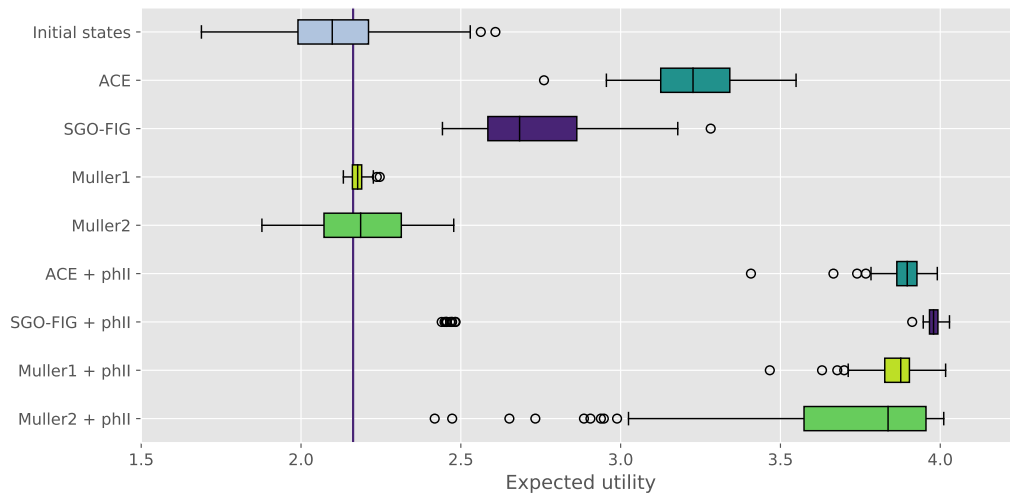


Figure 2: Expected utilities of designs returned by various optimal design algorithms methods for the pharmacokinetic example. Each method was run from the same set of 100 randomly sampled initial designs. The same initial designs are reused for each method. The bottom four rows show results after post-processing with ACE phase II. For each returned design, the expected utility was calculated via a Monte Carlo estimate using 2×10^4 utility evaluations to allow for a fair comparison. A box plot showing the expected utility at the initial designs is included for comparison, as well as a vertical line giving expected utility of a uniformly spaced design over the search space.

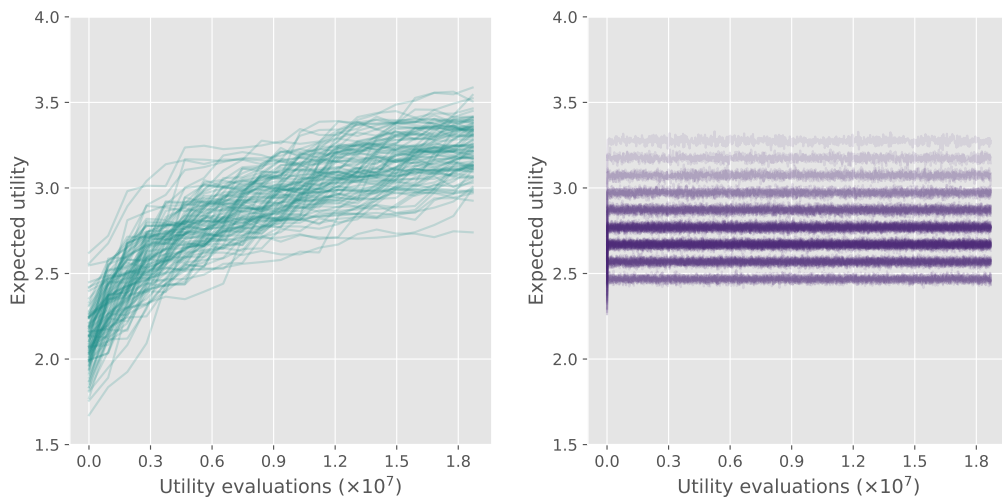


Figure 3: Trace plots of expected utility for the pharmacokinetic example using (a) ACE and (b) SGO-FIG. Traces are shown for 100 randomly sampled initial designs. The same initial designs are reused for each method. The expected utility estimates shown for ACE are by-products of its other calculations. Those for SGO-FIG are averages of utility estimates from recent steps of Algorithm 1. Darker lines in (b) correspond to more frequent trace paths.

space. SGO-FIG converges to designs that have repeated observations at times close to 1 and 8. Across the 100 runs only the proportions at these two times change, indicating these designs are local maxima. ACE also returns designs where all times are close to 1 and 8. However there is more variability in the observation times, suggesting that these algorithms have not yet converged to a local maximum. Also, ACE places more observation times near to 1 than SGO-FIG. This suggests it is better at avoiding poor local maxima.

Post-processing usually selects all observation times to be close to 1 rather than close to 8. Since post-processing improves the expected utility, as shown by Figure 2, it appears that this is the optimal design. The SGO-FIG algorithm has 10 runs where the design returned places all observations around 8, and post-processing cannot move points to other times to improve the utility. These correspond to the outlying points in Figure 2 where SGO-FIG plus post-processing achieves a poor expected utility close to 2.5.

We also investigate different choices of batch size K in SGO-FIG. The trace plots in Figure 5 show that for $K = 1, 10$ or 100 , SGO-FIG converges in roughly the same number of iterations ($\approx 10^4$). Hence $K = 1$ is most efficient in terms of computational cost.

Summary Our simulation study shows that FIG is much quicker to compute than SIG. Furthermore, SGO-FIG finds utility maxima using fewer utility evaluations than the other algorithms investigated. However it is slower than ACE in terms of time taken to run a fixed number of utility evaluations. Overall, this does not prevent SGO-FIG from being quicker to converge to its final design. We expect the advantage to be more pronounced in examples with more expensive utility evaluations.

SGO-FIG is more susceptible than ACE to finding poor local maxima. However combining SGO-FIG with a post-processing by ACE phase II usually finds the global maximum. In a small number of cases the SGO-FIG designs reach a local maximum that the post-processing algorithm could not improve significantly.

Overall we found SGO-FIG followed by post-processing was the most efficient way to find the global maximum. However multiple runs are required to avoid the possibility of being stuck at a local maximum.

The optimal design in this setting is somewhat counter-intuitive – all observations are made at the same time! However it has been argued that

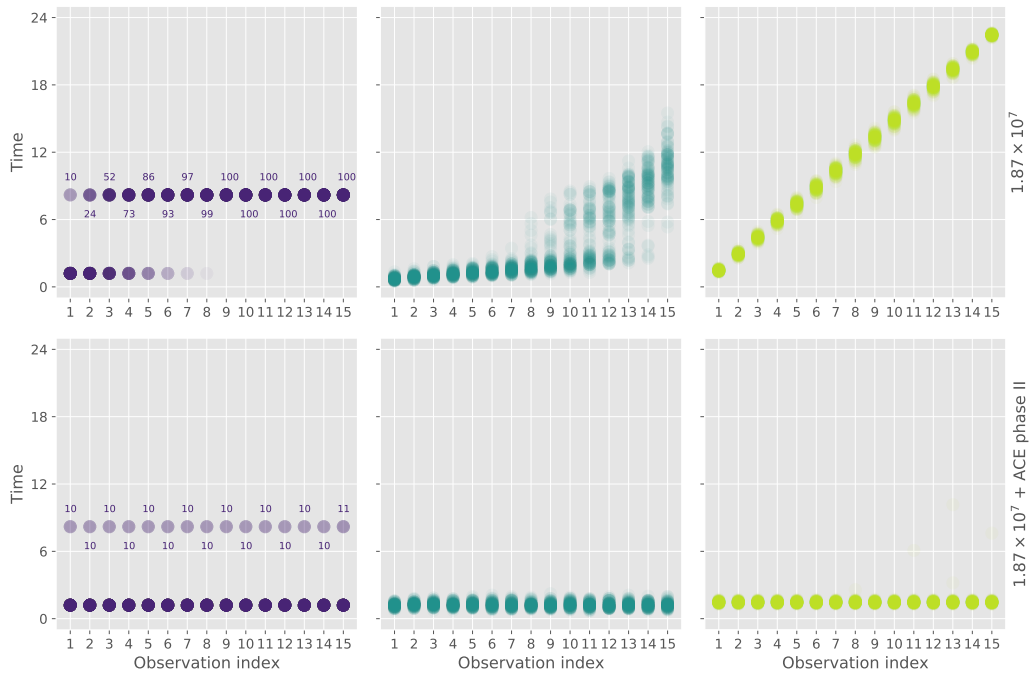


Figure 4: Designs returned by different optimal design methods for the pharmacokinetic example (a) SGO-FIG (b) ACE (c) Müller. Designs are shown for 100 randomly sampled initial designs. The same initial designs are reused for each method. Each design is sorted in increasing order. Darker points indicate higher frequencies of observations around a particular time. For SGO-FIG, text labels have been added to make the frequencies clearer.

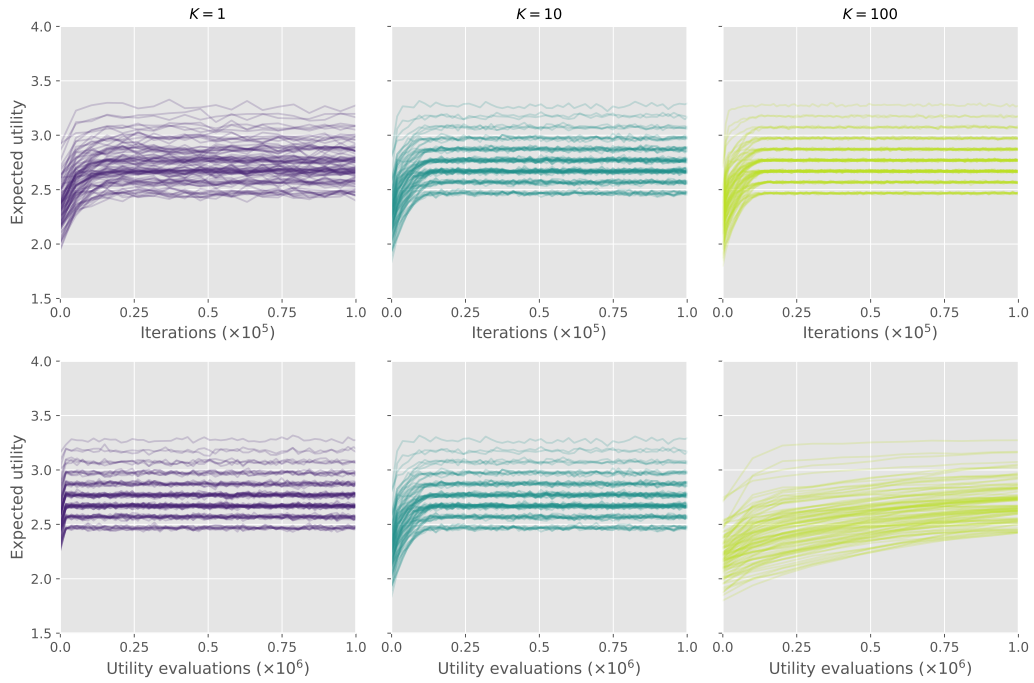


Figure 5: Trace plots of SGO-FIG for the pharmacokinetic example using various choices of batch size K . Traces are shown for 100 randomly sampled initial designs. The same initial designs are reused for each method. The expected utilities estimates shown are averages of utility estimates from recent steps of Algorithm 1. The top row shows number of SGO-FIG iterations on the x -axis and the bottom row instead shows number of utility evaluations.

replicated observation times can be highly informative (Binois et al., 2019). We discuss to what extent our choice of utility encourages replication in Section 8.

7 Geostatistical regression example

This section investigates an example requiring hundreds of design choices, to investigate how our method scales up to higher dimensional applications.

Model Consider the following geostatistical regression model. Here a design τ is a $d \times 2$ matrix whose i th row specifies the location of a measurement. (For the purposes of running the optimal design algorithms, τ can be flattened into a vector.) The model assumes normal observations with a linear trend and squared exponential covariance function with a nugget effect, giving

$$y \sim N(x(\theta, \tau), \Sigma(\tau)), \quad x_i = \theta_1 \tau_{i1} + \theta_2 \tau_{i2},$$

$$\Sigma = \sigma_1^2 I + \sigma_2^2 R(\tau), \quad R_{ij} = \exp \left[- \sum_{k=1}^2 (\tau_{ik} - \tau_{jk})^2 / \ell^2 \right].$$

For simplicity we assume that σ_1^2, σ_2^2 (observation variance components) and ℓ (covariance length scale) are known. Hence the unknown parameters are θ_1 and θ_2 (trends). An alternative parameterisation which will be useful shortly introduces $\kappa = \sigma_1^2 + \sigma_2^2$ and $\gamma = \sigma_1^2 / (\sigma_1^2 + \sigma_2^2)$ so that $\Sigma = \kappa[\gamma I + (1 - \gamma)R]$.

FIG utility Using (11) the FIG utility is,

$$\text{tr } \mathcal{I}(\tau) = \sum_{i=1}^d \tau_i^T \Sigma(\tau)^{-1} \tau_i,$$

where τ_i is the i th row of τ . Note that in this setting the FIG does not depend on θ . Hence $\mathcal{J}_{FIG}(\tau)$ simply equals $\text{tr } \mathcal{I}(\tau)$. Also note that κ only affects \mathcal{J}_{FIG} as a constant of proportionality, so it does not change the optimal design. (Recall Remark 3 – changing Σ to $\kappa\Sigma$ does not affect the optimal design.)

Simulation study We performed various simulation studies to search for $d = 100$ design locations restricted to a unit square centred at the origin.

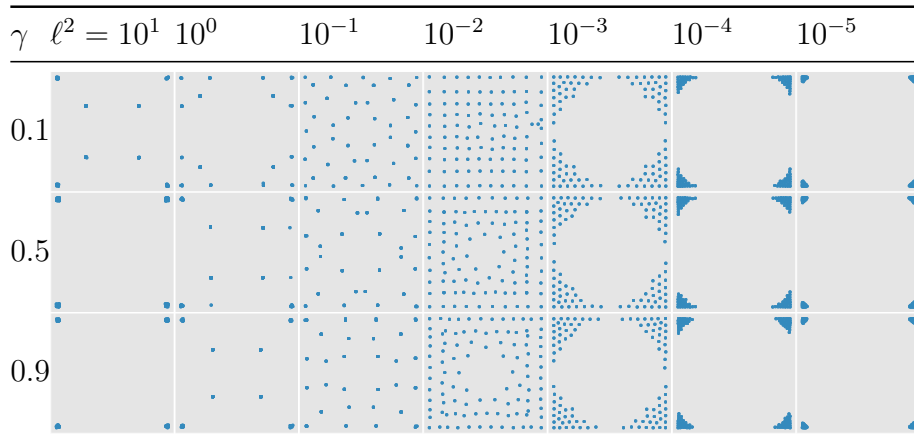


Figure 6: Geostatistical regression model designs returned by SGO-FIG for various choices of γ and ℓ . The design space is a unit square centred at the origin.

Throughout we use Algorithm 1, with a batch size of $K = 1$. We implemented constrained optimisation by adding a large L_1 penalty to designs outside the unit square. Adaptive weights were not considered as the contributions of the parameters to the expected utility are similar by symmetry. Also for simplicity we did not post-process the results, although this may improve the designs in cases where the design points fall into a few small clusters.

Figure 6 shows resulting designs under various choices of γ and ℓ . For both large and small ℓ values, the design points cluster in the corners. In between these extremes, the points are more uniformly spaced in the unit square.

For a comparison with ACE we fix $\gamma = 0.1$ and $\ell^2 = 10^{-3}$. Both algorithms were started from 100 initial designs sampled uniformly over the design space. For fair comparison, the initial designs used were common to both algorithms. The default settings for ACE were used, noting that the expected utility is deterministic so it was not necessary to estimate it using Monte Carlo. SGO-FIG used 5×10^4 iterations and a batch size of $K = 1$. These settings result in computational budgets of $\approx 8.5 \times 10^4$ and 5×10^4 utility evaluations per run for ACE and SGO-FIG respectively. Each SGO-FIG run took roughly 45 seconds, while the ACE analyses took roughly 4 minutes each. Figure 7 shows that SGO-FIG converges after using many fewer utility evaluations than ACE, and returns designs with higher expected utility values.

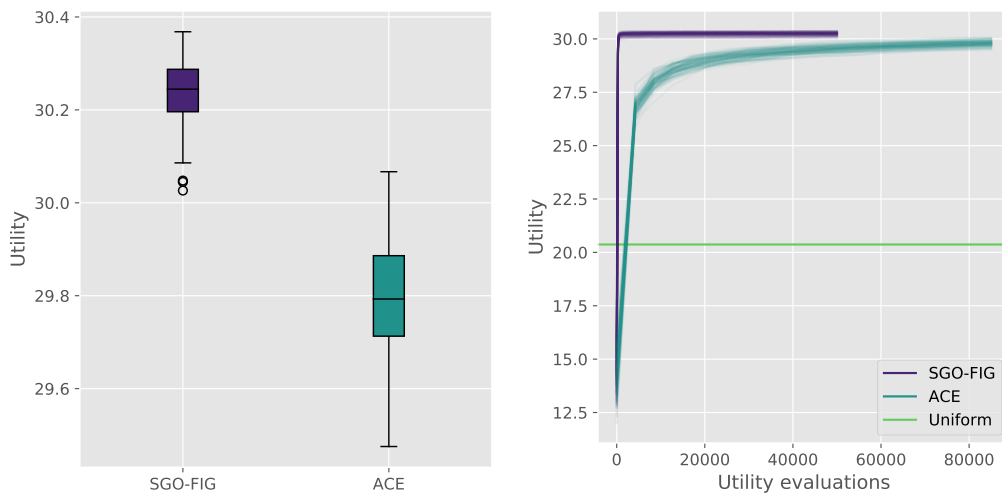


Figure 7: Comparison of optimal design algorithms for the geostatistical regression example. (a) Expected utilities of designs over 100 replications from different initial conditions. (b) Trace plots of the utility over the computation of the algorithms (generated as in Figure 3). The horizontal line indicates the utility for a uniformly spaced grid over the design space.

8 Discussion

We have presented a stochastic gradient optimisation algorithm, SGO-FIG, for Bayesian experimental design which can quickly find high dimensional designs under a particular fast-to-compute utility function, Fisher information gain. We also provide a novel decision theoretic justification for this utility. In our simulation studies SGO-FIG finds local maxima of the expected utility function faster than other state of the art methods. We ran our experiments on a CPU, but our Tensorflow code can easily make use of GPU parallelisation, allowing for further speed improvements.

Recommendations We recommend using SGO-FIG as follows. Perform multiple runs of SGO-FIG from random initial designs. If any of the resulting designs contain replicated points, then post-process using ACE phase II. Estimate the expected utility for each of the resulting designs and select the best performing.

Our recommended approach is motivated by one of our simulation studies (Section 6). Here SGO-FIG without post-processing typically converged to sub-optimal local maxima, but this was usually resolved by applying ACE phase II. Multiple runs are recommended as a small number of runs did not find the best design even after post-processing.

Future directions There may be scope for future work modifying generic stochastic gradient optimisation methods to avoid local maxima in optimal design problems e.g. using tempering methods, or non-local updates such as line search, as used in ACE.

In Section 6 we also observed that maximising the expected FIG often produces designs with repeated points. A similar finding was reported by Pronzato and Walter (1985). We speculate that the issue may be as follows. Repeated observation times can produce highly concentrated posteriors under some observed data, at the cost of less informative results otherwise. Overall the expected FIG rewards such trade-offs, as Fisher information is an approximation to posterior precision. In other words, FIG can be viewed as a *risk seeking* utility function. (For more on risk attitudes of utility functions see e.g. French and Insua, 2000.) This suggests modifying the utility to give decreasing returns to posterior concentration – e.g. using a utility $\log \text{tr} \mathcal{I}(\theta; \tau)$ – effectively introducing more risk aversion. It would be interesting to explore

whether there are variations on the FIG along these lines which avoid designs with repeated points while retaining its computational convenience and decision theoretic support.

More generally, stochastic gradient optimisation could also be used for other utility functions whose gradients can be calculated, such as other functionals of the Fisher information matrix e.g. $\det \mathcal{I}(\theta; \tau)$ and $\text{tr} \mathcal{I}(\theta; \tau)^{-1}$. However the cost of computing determinants or inverses of $\mathcal{I}(\theta; \tau)$ is higher than simply computing the trace, and there is arguably less theoretical backing for these utility functions.

Acknowledgements

The authors thank Kevin Wilson, Chris Oates, John Matthews and Philip Dawid for helpful conversations, and gratefully acknowledge an EPSRC studentship supporting Sophie Harbisher.

References

- Abadi, M. et al. (2016). Tensorflow: A system for large-scale machine learning. In *12th USENIX Symposium on Operating Systems Design and Implementation (OSDI 16)*, pages 265–283.
- Amzal, B., Bois, F. Y., Parent, E., and Robert, C. P. (2006). Bayesian-optimal design via interacting particle systems. *Journal of the American Statistical Association*, 101(474):773–785.
- Baydin, A. G., Pearlmutter, B. A., Radul, A. A., and Siskind, J. M. (2017). Automatic differentiation in machine learning: a survey. *Journal of Machine Learning Research*, 18(153):1–153.
- Bernardo, J. M. (1979). Expected information as expected utility. *The Annals of Statistics*, 7(3):686–690.
- Binmore, K. (2007). *Playing for real: a text on game theory*. Oxford university press.
- Binois, M., Huang, J., Gramacy, R. B., and Ludkovski, M. (2019). Replication or exploration? Sequential design for stochastic simulation experiments. *Technometrics*, 61(1):7–23.

- Bottou, L., Curtis, F. E., and Nocedal, J. (2018). Optimization methods for large-scale machine learning. *Siam Review*, 60(2):223–311.
- Box, G. E. P. (1982). Choice of response surface design and alphabetic optimality. *Utilitas Math. B*, 21:11–55.
- Chaloner, K. and Verdinelli, I. (1995). Bayesian experimental design: A review. *Statistical Science*, pages 273–304.
- Cook, A. R., Gibson, G. J., and Gilligan, C. A. (2008). Optimal observation times in experimental epidemic processes. *Biometrics*, 64(3):860–868.
- Figurnov, M., Mohamed, S., and Mnih, A. (2018). Implicit reparameterization gradients. In *Advances in Neural Information Processing Systems*, pages 441–452.
- French, S. and Insua, D. R. (2000). *Statistical decision theory*. Wiley.
- Gillespie, C. S. and Boys, R. J. (2019). Efficient construction of Bayes optimal designs for stochastic process models. *Statistics and Computing (online preview)*.
- Gneiting, T. and Raftery, A. E. (2007). Strictly proper scoring rules, prediction, and estimation. *Journal of the American Statistical Association*, 102(477):359–378.
- Huan, X. and Marzouk, Y. M. (2013). Simulation-based optimal Bayesian experimental design for nonlinear systems. *Journal of Computational Physics*, 232(1):288–317.
- Huan, X. and Marzouk, Y. M. (2014). Gradient-based stochastic optimization methods in Bayesian experimental design. *International Journal for Uncertainty Quantification*, 4(6).
- Hyvärinen, A. (2005). Estimation of non-normalized statistical models by score matching. *Journal of Machine Learning Research*, 6:695–709.
- Jankowiak, M. and Obermeyer, F. (2018). Pathwise derivatives beyond the reparameterization trick. In *International Conference on Machine Learning*, pages 2240–2249.

- Kingma, D. P. and Ba, J. (2015). Adam: A method for stochastic optimization. *International Conference on Learning Representations*.
- Krause, A., Rajagopal, R., Gupta, A., and Guestrin, C. (2009). Simultaneous placement and scheduling of sensors. In *Proceedings of the 2009 International Conference on Information Processing in Sensor Networks*, pages 181–192. IEEE Computer Society.
- Küick, H., de Freitas, N., and Doucet, A. (2006). SMC samplers for Bayesian optimal nonlinear design. In *2006 IEEE Nonlinear Statistical Signal Processing Workshop*, pages 99–102. IEEE.
- Kushner, H. and Yin, G. G. (2003). *Stochastic approximation and recursive algorithms and applications*. Springer Science & Business Media.
- Lindley, D. (1972). *Bayesian statistics, a review*. SIAM.
- Maddison, C. J., Mnih, A., and Teh, Y. W. (2017). The concrete distribution: A continuous relaxation of discrete random variables. *International Conference on Learning Representations*.
- Mescheder, L., Nowozin, S., and Geiger, A. (2017). The numerics of GANs. In *Advances in Neural Information Processing Systems*, pages 1825–1835.
- Miller, K. S. (1974). *Complex stochastic processes: an introduction to theory and application*. Addison Wesley Publishing Company.
- Müller, P. (1999). Simulation-based optimal design. In *Bayesian Statistics 6: Proceedings of Sixth Valencia International Meeting*, pages 459–474. Oxford University Press.
- Oates, C. J., Cockayne, J., Prangle, D., Sullivan, T. J., and Girolami, M. (2019). Optimality criteria for probabilistic numerical methods. *arXiv preprint arXiv:1901.04326*.
- Overstall, A., Woods, D., and Adamou, M. (2017). acebayes: An R package for Bayesian optimal design of experiments via approximate coordinate exchange. *arXiv preprint arXiv:1705.08096*.
- Overstall, A. M. and Woods, D. C. (2017). Bayesian design of experiments using approximate coordinate exchange. *Technometrics*, 59(4):458–470.

- Parry, M., Dawid, A. P., and Lauritzen, S. (2012). Proper local scoring rules. *The Annals of Statistics*, 40(1):561–592.
- Price, D. J., Bean, N. G., Ross, J. V., and Tuke, J. (2018). An induced natural selection heuristic for finding optimal Bayesian experimental designs. *Computational Statistics & Data Analysis*, 126:112–124.
- Pronzato, L. and Walter, É. (1985). Robust experiment design via stochastic approximation. *Mathematical Biosciences*, 75(1):103–120.
- Raiffa, H. and Schlaifer, R. (1961). *Applied statistical decision theory*. Division of Research, Harvard Business School.
- Renshaw, E. (1993). *Modelling Biological Populations in Space and Time*. Cambridge University Press.
- Rezende, D. J., Mohamed, S., and Wierstra, D. (2014). Stochastic back-propagation and approximate inference in deep generative models. In *International Conference on Machine Learning*, pages 1278–1286.
- Ruder, S. (2016). An overview of gradient descent optimization algorithms. *arXiv preprint arXiv:1609.04747*.
- Ryan, E. G., Drovandi, C. C., McGree, J. M., and Pettitt, A. N. (2016). A review of modern computational algorithms for Bayesian optimal design. *International Statistical Review*, 84(1):128–154.
- Ryan, E. G., Drovandi, C. C., Thompson, M. H., and Pettitt, A. N. (2014). Towards Bayesian experimental design for nonlinear models that require a large number of sampling times. *Computational Statistics & Data Analysis*, 70:45–60.
- Shewry, M. C. and Wynn, H. P. (1987). Maximum entropy sampling. *Journal of applied statistics*, 14(2):165–170.
- Walker, S. G. (2016). Bayesian information in an experiment and the Fisher information distance. *Statistics & Probability Letters*, 112:5–9.
- Wolfson, L. J., Kadane, J. B., and Small, M. J. (1996). Expected utility as a policy-making tool: an environmental health example. *Statistics Textbooks and Monographs*, 151:261–278.

A Decision theoretic support

This appendix justifies Result 1 of the main text i.e. the procedure of selecting the design maximising expected Fisher information gain can be derived from Bayesian decision theory. Our argument extends that of Bernardo (1979), who gives a decision theoretic derivation for maximising expected Shannon information gain. First Section A.1 reviews background material on scoring rules. Section A.2 proves a general result linking scoring rules and utilities in experimental design. Then Section A.3 relates this result to Shannon information gain and Section A.4 to Fisher information gain, proving Result 1.

A.1 Scoring rules

A *scoring rule* $S(q, \theta)$ measures the quality of a distribution to model an uncertain quantity, given a realised value θ . For the purposes of this paper we represent the distribution by its density $q(\theta)$. Low scores represent a good match.

A scoring rule is *strictly proper* if it is always true that $\mathbb{E}_{\theta \sim p(\theta)}[S(q, \theta)]$ is uniquely minimised by $q = p$. An interpretation of this property is as follows. Consider a decision problem where a density q must be reported for a quantity $\theta \sim p(\theta)$ and the loss function is a scoring rule. The scoring rule is strictly proper if and only if the action minimising expected loss is to report the actual density, $p(\theta)$. The expected loss resulting from this action is referred to as the *entropy*,

$$\mathcal{H}[p(\theta)] = \mathbb{E}_{\theta \sim p(\theta)}[S(p(\theta), \theta)].$$

The extra expected loss from making a non-optimal action q is known as the *divergence*,

$$\mathcal{D}[p(\theta), q(\theta)] = \mathbb{E}_{\theta \sim p(\theta)}[S(q(\theta), \theta) - S(p(\theta), \theta)].$$

Table 3 summarises the quantities just described for two strictly proper scoring rules, logarithmic score and Hyvärinen score (Hyvärinen, 2005). The Hyvärinen results rely on the following regularity conditions:

1. $p(\theta)$ and $q(\theta)$ are twice differentiable with respect to all θ_i .
2. $\mathbb{E}_{\theta \sim p(\theta)}[\|\nabla \log p(\theta)\|^2]$, $\mathbb{E}_{\theta \sim q(\theta)}[\|\nabla \log q(\theta)\|^2]$ are finite.

	Logarithmic score	Hyvärinen score
Scoring rule	$-\log q(\theta)$	$2\Delta \log q(\theta) + \ \nabla \log q(\theta)\ ^2$
Entropy	$-\mathbb{E}_{\theta \sim p(\theta)}[\log p(\theta)]$	$-\mathbb{E}_{\theta \sim p(\theta)}[\ \nabla \log p(\theta)\ ^2]$
Divergence	$\mathbb{E}_{\theta \sim p(\theta)}[\log p(\theta) - \log q(\theta)]$	$\mathbb{E}_{\theta \sim p(\theta)}[\ \nabla \log p(\theta) - \nabla \log q(\theta)\ ^2]$

Table 3: Summary of two scoring rules and related quantities. Here $p(\theta)$ is the true density of an unobserved quantity and $q(\theta)$ is a generic density. Note that Δ is the Laplacian operator (sum of second partial derivatives). For a derivation of the Hyvärinen divergence see Appendix A of Hyvärinen (2005). The other derivations are straightforward.

3. $\nabla p(\theta) \rightarrow 0, \nabla q(\theta) \rightarrow 0$ for $\|\theta\| \rightarrow \infty$.

Throughout this appendix ∇ represents gradient with respect to θ , and $\|\theta\|$ represents the L_2 norm i.e. $\|x\| = \sqrt{x^T x}$.

For more discussion of scoring rules see for example Gneiting and Raftery (2007) and Parry et al. (2012).

A.2 General result

Recall the Bayesian decision theory framework of Section 2.3. After picking a design τ and observing data y , the experimenter must take an action a . They then receive some base utility $\mathcal{V}(a, \theta, y, \tau)$, involving the true parameter value θ . Their utility \mathcal{U} for the design τ given data y is

$$\mathcal{U} = \max_a \mathbb{E}_{\theta \sim \pi(\theta|y;\tau)}[\mathcal{V}(a, \theta, y, \tau)].$$

i.e. the expected base utility under the posterior distribution for θ , assuming that the optimal a is selected. (Throughout this appendix \mathcal{U} has arguments τ, y , but these are suppressed to simplify notation.)

Following Bernardo (1979), suppose that a is an estimated density for θ . Let the base utility be the negative of a strictly proper scoring rule. Then, by the discussion in the previous section, the experimenter's utility \mathcal{U} is the negative of the entropy associated with the scoring rule, evaluated on $\pi(\theta|y; \tau)$.

The following lemma shows that two other utility functions produce equivalent expected utilities to the negative entropy. The proof is based on

the common observation that the divergence contains a constant term which can be ignored under maximisation. Similar results have appeared in the experimental design literature previously for a logarithmic score function (e.g. Shewry and Wynn, 1987). This lemma simply generalises them to a general score function.

Lemma 1. *Given an underlying strictly proper score function S , the following choices of utility function produce the same expected utility in Bayesian experimental design:*

$$\mathcal{U}_{\text{entropy diff}} = \mathcal{H}[\pi(\theta)] - \mathcal{H}[\pi(\theta|y; \tau)], \quad \mathcal{U}_{\text{divergence}} = \mathcal{D}[\pi(\theta|y; \tau), \pi(\theta)].$$

Furthermore the utility

$$\mathcal{U}_{\text{entropy}} = -\mathcal{H}[\pi(\theta|y; \tau)]$$

produces the same expected utility up to an additive constant and hence shares the same optimal design.

Proof. In the framework of Section 2, Bayesian experimental design is concerned with optimising the expected utility $\mathbb{E}_{\theta, y \sim \pi(\theta, y)}[\mathcal{U}]$ where $\pi(\theta, y) = \pi(\theta)f(y|\theta; \tau)$. Using (2) and (3), we also have $\pi(\theta, y) = \pi(\theta|y; \tau)\pi(y; \tau)$.

From the definitions of Section A.1,

$$\mathcal{U}_{\text{divergence}} = \mathcal{U}_{\text{entropy}} + \mathbb{E}_{\theta \sim \pi(\theta|y; \tau)}[S(\pi(\theta), \theta)].$$

Hence

$$\begin{aligned} \mathbb{E}_{(\theta, y) \sim \pi(\theta, y)}[\mathcal{U}_{\text{divergence}}] &= \mathbb{E}_{(\theta, y) \sim \pi(\theta, y)}[\mathcal{U}_{\text{entropy}}] + \mathbb{E}_{(\theta, y) \sim \pi(\theta, y)}[S(\pi(\theta), \theta)] \\ &= \mathbb{E}_{(\theta, y) \sim \pi(\theta, y)}[\mathcal{U}_{\text{entropy diff}}]. \end{aligned}$$

So $\mathcal{U}_{\text{divergence}}$ and $\mathcal{U}_{\text{entropy diff}}$ produce the same expected utility. Furthermore the expected utility of $\mathcal{U}_{\text{entropy}}$ only differs by an additive constant, since $\mathbb{E}_{(\theta, y) \sim \pi(\theta, y)}[S(\pi(\theta), \theta)]$ does not depend on τ . \square

A.3 Logarithmic score and Shannon information gain

In the case of the logarithmic score function the equivalent utilities from Lemma 1 are

$$\begin{aligned} \mathcal{U}_{\text{entropy}} &= \mathbb{E}_{\theta \sim \pi(\theta|y; \tau)}[\log \pi(\theta|y; \tau)], \quad (\text{negative Shannon entropy}) \\ \mathcal{U}_{\text{entropy diff}} &= \mathbb{E}_{\theta \sim \pi(\theta|y; \tau)}[\log \pi(\theta|y; \tau)] - \mathbb{E}_{\theta \sim \pi(\theta)}[\log \pi(\theta)], \\ \mathcal{U}_{\text{divergence}} &= \mathbb{E}_{\theta \sim \pi(\theta|y; \tau)}[\log \pi(\theta|y; \tau) - \log \pi(\theta)]. \quad (\text{Kullback-Leibler divergence}) \end{aligned}$$

Another equivalent utility is the quantity within the expectation in $\mathcal{U}_{\text{divergence}}$,

$$\mathcal{U}_{\text{SIG}} = \log \pi(\theta|y; \tau) - \log \pi(\theta),$$

which is the Shannon information gain (6). Hence Lemma 1 provides decision theoretic support for this utility. It does so by essentially following the argument of Bernardo (1979).

A.4 Hyvärinen score and Fisher information gain

Under the Hyvärinen score function the equivalent utilities from Lemma 1 are

$$\begin{aligned} \mathcal{U}_{\text{entropy}} &= \mathbb{E}_{\theta \sim \pi(\theta|y; \tau)} [|\nabla \log \pi(\theta|y; \tau)|^2], \\ \mathcal{U}_{\text{entropy diff}} &= \mathbb{E}_{\theta \sim \pi(\theta|y; \tau)} [|\nabla \log \pi(\theta|y; \tau)|^2] - \mathbb{E}_{\theta \sim \pi(\theta)} [|\nabla \log \pi(\theta)|^2], \\ \mathcal{U}_{\text{divergence}} &= \mathbb{E}_{\theta \sim \pi(\theta|y; \tau)} [|\nabla \log \pi(\theta|y; \tau) - \nabla \log \pi(\theta)|^2]. \end{aligned}$$

Two further equivalent utilities are the quantity within the expectation in $\mathcal{U}_{\text{divergence}}$,

$$\mathcal{U}_{\text{score diff}} = \|\nabla \log \pi(\theta|y; \tau) - \nabla \log \pi(\theta)\|^2 = \|\nabla \log f(y|\theta; \tau)\|^2,$$

and its expectation

$$\mathcal{U}_{\text{FIG}} = \mathbb{E}_{y \sim f(y|\theta; \tau)} [|\nabla \log f(y|\theta; \tau)|^2],$$

i.e. the trace of the Fisher information. This argument proves Result 1 from the main text. We refer to \mathcal{U}_{FIG} as Fisher information gain in a rough analogy to Shannon information gain. While a closer analogy would be to refer to $\mathcal{U}_{\text{score diff}}$ as Fisher information gain, we prefer to reserve the term for the more computationally convenient form \mathcal{U}_{FIG} .

Walker (2016) proved directly that \mathcal{U}_{FIG} , $\mathcal{U}_{\text{entropy diff}}$ and $\mathcal{U}_{\text{divergence}}$ give the same expected utility. We have shown that the same result arises naturally from a decision theory characterisation.

B Adaptive weights algorithm

Here we present our algorithm for adaptively maximising the weighted FIG utility (14), while learning suitable weights. We also describe the motivation behind the algorithm, and examine its convergence properties.

As discussed in Section 4.4, (14) is equivalent to scaling each parameter θ_i by a weight w_i . For notational convenience below, we introduce $\tilde{w}_i = w_i^2$ and let \tilde{w} be the corresponding vector of squared weights. The weighted FIG can then be written

$$\mathcal{U}_{FIG}(\tau, \theta, y; \tilde{w}) = \text{diag}(\mathcal{I}(\theta; \tau))^T \tilde{w}^{-1} = \sum_{i=1}^p \mathbb{E}_{y \sim f(y|\theta; \tau)} [u_i(y, \theta; \tau)^2 / \tilde{w}_i],$$

where diag maps a matrix to its leading diagonal and \tilde{w}^{-1} is the vector of \tilde{w}_i^{-1} values. The resulting expected utility is $\mathcal{J}_{FIG}(\tau; \tilde{w}) = \mathbb{E}_{\theta \sim \pi(\theta)} [\mathcal{U}_{FIG}(\tau, \theta, y; \tilde{w})]$.

As discussed in Section 4.4, we wish to select (1) a design maximising the weighted FIG utility and (2) weights which give each parameter give an equal contribution to $\mathcal{J}_{FIG}(\tau; \tilde{w})$. More precisely, our goal is to find (τ^*, \tilde{w}^*) such that:

1. τ^* maximises $\mathcal{J}_{FIG}(\tau; \tilde{w}^*)$,
2. $\tilde{w}^* = g(\tau^*)$ where $g(\tau) = \mathbb{E}_{\theta \sim \pi(\theta)} [\text{diag}(\mathcal{I}(\theta; \tau^*))]$.
Equivalently, \tilde{w}^* maximises $\mathcal{K}(\tilde{w}; \tau^*)$ where

$$\mathcal{K}(\tilde{w}; \tau) = -\frac{1}{2} \|\tilde{w} - g(\tau)\|^2.$$

Algorithm 2 is an algorithm for optimal design with adaptive weights. It operates by applying stochastic gradient optimisation updates to τ and w . An unbiased Monte Carlo gradient estimate of $\nabla_{\tau} \mathcal{J}_{FIG}(\tau; \tilde{w})$ is

$$\widehat{\nabla \mathcal{J}_{FIG}}(\tau; \tilde{w}) = \frac{1}{K} \sum_{k=1}^K \nabla [\text{diag}(\mathcal{I}(\theta^{(k)}; \tau))^T \tilde{w}^{-1}], \quad (15)$$

where $\theta^{(k)}$ are independent draws from the prior. This corresponds to (12) for the unweighted case.

An unbiased Monte Carlo gradient estimate of $\nabla_{\tilde{w}} \mathcal{K}(\tilde{w}; \tau)$ is

$$\widehat{\nabla \mathcal{K}}(\tilde{w}; \tau) = \frac{1}{K} \sum_{k=1}^K \text{diag}(\mathcal{I}(\theta^{(k)}; \tau)) - \tilde{w}. \quad (16)$$

The same $\theta^{(k)}$ draws used for (15) can be reused in (16).

Algorithm 2 Stochastic gradient optimisation of expected Fisher information gain with adaptive weights

Input: Initial design τ_0 , number of iterations n , batch size K to use in gradient estimation, initial squared weights \tilde{w}_0 .

Loop over $t = 0, 1, 2, \dots, n - 1$ or until a convergence condition is reached:

1. Calculate an estimated gradient for τ , using (15), and an estimated gradient for \tilde{w} , using (16).
2. Get $\tau_{t+1}, \tilde{w}_{t+1}$ by calling the update rule of a stochastic gradient optimisation algorithm with current state τ_t, \tilde{w}_t and gradient estimate from step 1. We use the update rule of the Adam algorithm.

Algorithm 2 can be viewed as a *simultaneous gradient ascent* approach as it make simultaneous gradient ascent steps for two objective functions. It is well known that such algorithms do not always converge (see e.g. Mescheder et al., 2017). The issue is that improving one objective function may reduce the other, resulting in dynamics of (τ_t, \tilde{w}_t) which form a cycle rather than converging to an optimum. Furthermore, it is difficult to guarantee the existence of a solution to our adaptive optimisation problem, as discussed in Section B.1. Nonetheless we find reasonable performance of the algorithm in a simulation study (see Table 1). Also, as mentioned in the main text, the algorithm can be used simply to select reasonable weights i.e. increase the value of $\mathcal{K}(\tilde{w}; \tau)$ compared to using unit weights. Then Algorithm 1 can be run on parameters rescaled by these weights.

B.1 Existence of a solution

Lemma 2 shows that a solution to the adaptive weights optimisation problem described above can be guaranteed under a few conditions. However one of these, item 4, is hard to verify: $h(\tilde{w})$, the solution to a maximisation problem defined by \tilde{w} , must be a continuous function of \tilde{w} . Therefore it is difficult to guarantee the existence of a solution in practice.

Lemma 2. *There exists a solution to*

$$\tau^* = \operatorname{argmax}_{\tau} \mathcal{J}_{FIG}(\tau; \tilde{w}^*), \quad \tilde{w}^* = \operatorname{argmax}_{\tilde{w}} \mathcal{K}(\tilde{w}; \tau^*)$$

given the following conditions:

1. The set $\mathcal{T} \subseteq \mathbb{R}^d$ of possible designs is compact and convex.
2. $g(\tau)$ is continuous.
3. $\|g(\tau)\|$ is bounded above.
4. There exists a continuous function $h(\tilde{w})$ outputting a τ value maximising $\mathcal{J}_{FIG}(\tau; \tilde{w})$.

The joint optimisation problem here is equivalent to the definition of a Nash equilibrium in game theory. To prove existence of a solution we follow the game theory literature by using Brouwer's fixed point theorem (see e.g. Binmore, 2007).

Proof. Let $\mathcal{W} = \{\tilde{w} \mid \|\tilde{w}\| \leq k\}$ where k is an upper bound of $\|g(\tau)\|$. Define $f : \mathcal{T} \times \mathcal{W} \rightarrow \mathcal{T} \times \mathcal{W}$ by $f(\tau, \tilde{w}) = (h(\tilde{w}), g(\tau))$. It follows from the assumptions that this is a continuous function from a compact convex set to itself. Hence by Brouwer's fixed point theorem, there exists some $(\tau^*, \tilde{w}^*) \in \mathcal{T} \times \mathcal{W}$ which is a fixed point of f . Therefore $\tau^* = h(\tilde{w}^*)$ and $\tilde{w}^* = g(\tau^*)$ as required. \square

C Fisher information gain for the pharmacokinetic example

Recall from Section 3.2 that for a model $y \sim N(x(\theta, \tau), \Sigma(\tau))$,

$$\text{tr } \mathcal{I}(\theta; \tau) = \sum_{i=1}^p v_i(\theta, \tau)^T \Sigma(\tau)^{-1} v_i(\theta, \tau)$$

where v_i is the vector $\frac{\partial}{\partial \theta_i} x(\theta, \tau)$ of elementwise derivatives of x . For the pharmacokinetic model $\Sigma = \sigma^2 I$ so that

$$\text{tr } \mathcal{I}(\theta; \tau) = \sigma^{-2} \sum_{i=1}^3 \sum_{j=1}^n v_{ij}(\theta, \tau)^2.$$

where $v_{ij} = \frac{\partial}{\partial \theta_i} x(\theta, \tau_j)$. It remains to compute the v_{ij} terms, which are

$$\begin{aligned} v_{1j} &= \frac{1}{\theta_2 - \theta_1} x(\theta, \tau_j) - \frac{D\theta_2}{\theta_3(\theta_2 - \theta_1)} \tau_j \exp(-\theta_1 \tau_j), \\ v_{2j} &= \frac{\theta_1}{\theta_2(\theta_1 - \theta_2)} x(\theta, \tau_j) + \frac{D\theta_2}{\theta_3(\theta_2 - \theta_1)} \tau_j \exp(-\theta_2 \tau_j), \\ v_{3j} &= -\frac{1}{\theta_3} x(\theta, \tau_j). \end{aligned}$$

D Regularity conditions

Under weak regularity conditions on $g(\theta, \tau)$ it is possible to interchange of differentiation and expectation so that

$$\nabla_\tau \mathbb{E}_{\theta \sim \pi(\theta)} [g(\theta, \tau)] = \mathbb{E}_{\theta \sim \pi(\theta)} [\nabla_\tau g(\theta, \tau)].$$

(This result was required in Section 4.2 with $g(\theta, \tau) = \text{tr } \mathcal{I}(\theta; \tau)$.) A sufficient regularity condition is that $\mathbb{E}_{\theta \sim \pi(\theta)} [|\nabla g(\theta, \tau)|]$ is finite, where absolute value $|\cdot|$ acts elementwise. It follows that interchange is possible by Fubini's theorem.

E More on estimation of FIG and its gradient

This appendix considers estimating the expected FIG utility, $\mathcal{J}_{FIG}(\tau)$, and its gradient when the Fisher information is not available in closed form. First note we can express

$$\mathcal{J}_{FIG}(\tau) = \mathbb{E}_{\theta \sim \pi(\theta), y \sim f(y|\theta; \tau)} [||u(y, \theta; \tau)||^2], \quad (17)$$

where u is the score function, (5). Hence a simple unbiased Monte Carlo estimate is

$$\frac{1}{K} \sum_{k=1}^K ||u(y^{(k)}, \theta^{(k)}; \tau)||^2.$$

where $(\theta^{(k)}, y^{(k)})$ are independent draws from the prior and model.

However, on taking the gradient of (17) with respect to τ , it is generally not possible to exchange the order of integration and differentiation. The reason is that the distribution for y depends on τ . This complicates obtaining a Monte Carlo estimate.

A standard approach is to use the “reparameterisation trick” (Rezende et al., 2014). The idea is to express y as a transformation $y(\epsilon, \theta, \tau)$ of a random variable ϵ with fixed density $p(\epsilon)$. Then

$$\mathcal{J}_{FIG}(\tau) = \mathbb{E}_{\theta \sim \pi(\theta), \epsilon \sim p(\epsilon)} [\|u(y(\epsilon, \theta, \tau), \theta; \tau)\|^2],$$

Now it is possible to exchange integration and differentiation under mild regularity conditions (see Appendix D) to get

$$\nabla \mathcal{J}_{FIG}(\tau) = \mathbb{E}_{\theta \sim \pi(\theta), \epsilon \sim p(\epsilon)} [\nabla \|u(y(\epsilon, \theta, \tau), \theta; \tau)\|^2].$$

Hence an unbiased Monte Carlo estimate is

$$\frac{1}{K} \sum_{k=1}^K [\nabla \|u(y(\epsilon^{(k)}, \theta^{(k)}, \tau), \theta^{(k)}; \tau)\|^2],$$

where $(\theta^{(k)}, \epsilon^{(k)})$ are independent draws from $\pi(\theta)p(\epsilon)$. Unbiased estimates of the quantities required for Algorithm 2 can be derived similarly.

In some cases y cannot be represented as a suitable transformation of ϵ . This includes the case of discrete y and other common distributions such as Beta and Gamma. Various techniques are available to deal with these cases such as taking a continuous approximation to discrete variables (Maddison et al., 2017) or using implicit differentiation (Figurnov et al., 2018; Jankowiak and Obermeyer, 2018).